Loss of autophagy causes a synthetic lethal deficiency in DNA repair

Emma Y. Liu[a], Naihan Xu[a,b], Jim O'Prey[a], Laurence Y. Lao[a], Sanket Joshi[a], Jaclyn S. Long[a], Margaret O'Prey[a], Daniel R. Croft[a], Florian Beaumatin[a], Alice D. Baudot[a], Michaela Mrschtik[a], Mathias Rosenfeldt[a], Yaou Zhang[b], David A. Gillespie[a,1], and Kevin M. Ryan[a,2]

[a]Cancer Research UK Beatson Institute, Glasgow G61 1BD, United Kingdom; and [b]Division of Life Science, Graduate School at Shenzhen, Tsinghua University, Shenzhen 518055, China

Edited by Eileen P. White, The Cancer Institute of New Jersey, New Brunswick, NJ, and accepted by the Editorial Board December 9, 2014 (received for review May 22, 2014)

(Macro)autophagy delivers cellular constituents to lysosomes for degradation. Although a cytoplasmic process, autophagy-deficient cells accumulate genomic damage, but an explanation for this effect is currently unclear. We report here that inhibition of autophagy causes elevated proteasomal activity leading to enhanced degradation of checkpoint kinase 1 (Chk1), a pivotal factor for the error-free DNA repair process, homologous recombination (HR). We show that loss of autophagy critically impairs HR and that autophagy-deficient cells accrue micronuclei and sub-G1 DNA, indicators of diminished genomic integrity. Moreover, due to impaired HR, autophagy-deficient cells are hyperdependent on nonhomologous end joining (NHEJ) for repair of DNA double-strand breaks. Consequently, inhibition of NHEJ following DNA damage in the absence of autophagy results in persistence of genomic lesions and rapid cell death. Because autophagy deficiency occurs in several diseases, these findings constitute an important link between autophagy and DNA repair and highlight a synthetic lethal strategy to kill autophagy-deficient cells.

autophagy | DNA repair | cell death | synthetic lethality

The preservation of genome integrity is critical for the prevention of human disease. In addition, the maintenance of proteome integrity is also considered central to healthy cellular homeostasis. Macroautophagy, hereafter referred to as autophagy, is a process that is paramount in counteracting damage to cytoplasmic constituents (1). Upon initiation of autophagy, double-membraned vesicles termed "autophagosomes" form to encapsulate cargoes including damaged or misfolded proteins and organelles. These vesicles ultimately fuse with lysosomes and the acidic hydrolases provided by the lysosome degrade cargoes into constituent parts, which can be recycled into biosynthetic pathways or in some situations, further catabolized to produce energy for the cell (1). Autophagy functions at basal levels in virtually all cells and is a major mechanism for protein turnover and the only known mechanism for degradation of organelles (1). Due to its crucial role in maintaining cytoplasmic and therefore cellular homeostasis, perturbations in autophagy have been reported to be an important contributing factor in a spectrum of diseases, including Crohn's disease, lysosomal storage disorders, neurodegenerative diseases, and cancer (2–6).

Autophagy operates in the cytoplasm and yet studies have shown that autophagy-deficient cells accumulate DNA damage (5). The reasons behind this observation, however, are not completely clear. Because the cellular environment of autophagy-deficient cells will cause accrual of damaged proteins with abnormal function and as a result accumulation of reactive oxygen species, it is easily conceivable that this will ultimately lead to a higher incidence of genetic lesions. However, even when autophagy is competent, our cells are already subject to an extremely high frequency of spontaneous DNA damage. The fact that this damage does not persist is due to highly efficient processes of DNA repair that serve to maintain genomic integrity (7, 8). We hypothesized, therefore, that the accumulation of genetic lesions in autophagy-deficient cells may be critically driven by a defect in DNA repair. We show that loss of autophagy leads to decreased levels of checkpoint kinase 1 (Chk1) and a greatly diminished ability to repair DNA double-strand breaks by homologous recombination (HR). As a result, autophagy-deficient cells are more reliant on nonhomologous end joining (NHEJ) for DNA repair, which uncovers a unique synthetic lethality-based strategy to kill cells that may be applicable to the treatment of various forms of human disease.

Results

Loss of Autophagy Leads to a Deficiency in the Kinase Chk1. To test if autophagy has a role in DNA repair, we wanted to use primary cell systems in which all DNA repair processes would be intact and within which autophagy could be rapidly eliminated immediately before exogenous, acutely induced DNA damage. We reasoned that in this context there would be limited time for accumulation of damaged proteins and reactive oxygen species that could lead to DNA damage and we would be able to assess directly the potential role of autophagy in DNA repair of lesions caused by exogenous agents. To this end, we designed

Significance

It is known that autophagy plays a major role in cellular homeostasis and impaired autophagy has been implicated in various forms of human disease. Here we investigate one way in which autophagy is critically connected to cellular integrity by showing that autophagy loss diminishes DNA repair by the error-free process, homologous recombination. As a result, this causes reliance on the error-prone process of nonhomologous end joining for repair of DNA double-strand breaks, providing one explanation of why autophagy-deficient cells accumulate genomic damage. These findings therefore have important implications for diseases in which autophagy is impaired and for therapeutic strategies designed to inhibit autophagy, particularly if autophagy inhibition is undertaken in combination with agents that cause genomic damage.

Author contributions: E.Y.L., N.X., D.A.G., and K.M.R. designed research; E.Y.L., N.X., J.O., L.Y.L., S.J., J.S.L., M.O., D.R.C., F.B., A.D.B., M.M., and K.M.R. performed research; J.O. and M.R. contributed new reagents/analytic tools; E.Y.L., N.X., J.O., L.Y.L., S.J., J.S.L., D.R.C., Y.Z., D.A.G., and K.M.R. analyzed data; and K.M.R. wrote the paper.

The authors declare no conflict of interest.

This article is a PNAS Direct Submission. E.P.W. is a guest editor invited by the Editorial Board.

Freely available online through the PNAS open access option.

[1]Present address: Centre for Biomedical Research of the Canary Islands, Department of Anatomy, Anatomical Pathology and Physiology/Faculty of Medicine, Universidad de La Laguna, 38071 Tenerife, Spain.

[2]To whom correspondence should be addressed. Email: k.ryan@beatson.gla.ac.uk.

This article contains supporting information online at www.pnas.org/lookup/suppl/doi:10.1073/pnas.1409563112/-/DCSupplemental.

an experimental system using primary mouse embryo fibroblasts (MEFs) from genetically modified mice that contain an essential autophagy gene flanked by loxP sites that can be targeted for recombination by Cre-recombinase (Cre) (Fig. S1*A*). MEFs were generated from *Atg7*$^{flox/flox}$ mice and were infected with either a retrovirus expressing Cre or empty retroviral vector as control. After 3 d of selection for infected cells, recombination of the Atg7 locus was confirmed by quantitative PCR (qPCR) (Fig. S1*B*) and both wild-type (*Atg7*$^{flox/flox}$) and *Atg7*$^{-/-}$ cells were exposed to 10 Gy ionizing irradiation (IR) to induce DNA double-strand breaks. At 1 h after irradiation, both cells exhibited a marked accumulation of phosphorylated histone 2AX (γ-H2AX) nuclear foci—a marker of DNA double-strand breaks (Fig. 1*A*). At later time points, both wild-type and *Atg7*$^{-/-}$ cells exhibited markedly fewer γ-H2AX foci and increased γ-H2AX could no longer be detected by Western blotting (Fig. 1 *A* and *B*), indicating that autophagy-deficient cells appear able to repair DNA double-strand breaks. To confirm this result, we also measured the ability of cells to resolve DNA damage more directly using the comet assay (9). This revealed, consistent with our γ-H2AX data, that wild-type and autophagy-deficient MEFs can repair DNA double-strand breaks at an equivalent rate (Fig. 1*C* and Fig. S1 *C* and *D*). The mechanism used for repair, however, cannot be determined by either the comet assay or analysis of γ-H2AX.

There are two principal mechanisms by which DNA double-strand breaks can be repaired: HR or NHEJ (10), and we were interested to know which mechanism was used in autophagy-deficient cells. DNA double-strand break repair via HR is error-free, whereas NHEJ is error-prone and can result in mutations and chromosome translocations (10). Because autophagy-deficient cells can repair DNA double-stand breaks and yet they are known to accumulate damage over time (5), we hypothesized that they use error-prone NHEJ instead of HR. We considered this may be because they have a defect in error-free HR and we decided to explore this possibility.

HR is a multistep process and we questioned whether autophagy-deficient cells were impaired at any point compared with wild-type controls. Resection of DNA double-strand breaks to reveal single-stranded DNA is a prerequisite for HR (11). CtIP is a protein required for DNA strand resection and the yeast ortholog of CtIP has been shown to be degraded by autophagy upon histone deacetylase inhibition (12). However, analysis for appearance of CtIP as nuclear foci following IR revealed no differences in CtIP foci in autophagy-deficient cells compared with controls (Fig. 1*D*).

Activation of the Chk1 kinase has also been shown to be critical for HR (13). We therefore measured phosphorylation of Chk1 at a site known to be phosphorylated by the kinase ATR (serine 345), which leads to activation of Chk1 following DNA damage (14). This measurement strikingly revealed that autophagy-deficient cells exhibit greatly diminished levels of phospho-Chk1 in response to IR (Fig. 1*E*). Similar results were also observed when cells were treated with the chemotherapeutic drug, etoposide, which also causes DNA double-strand breaks (Fig. 1*F*) (15). Moreover, at later time points after infection with Cre, total Chk1 as well as phospho-Chk1 was greatly diminished in the absence of Atg7 (Fig. 1*G*). Importantly, these

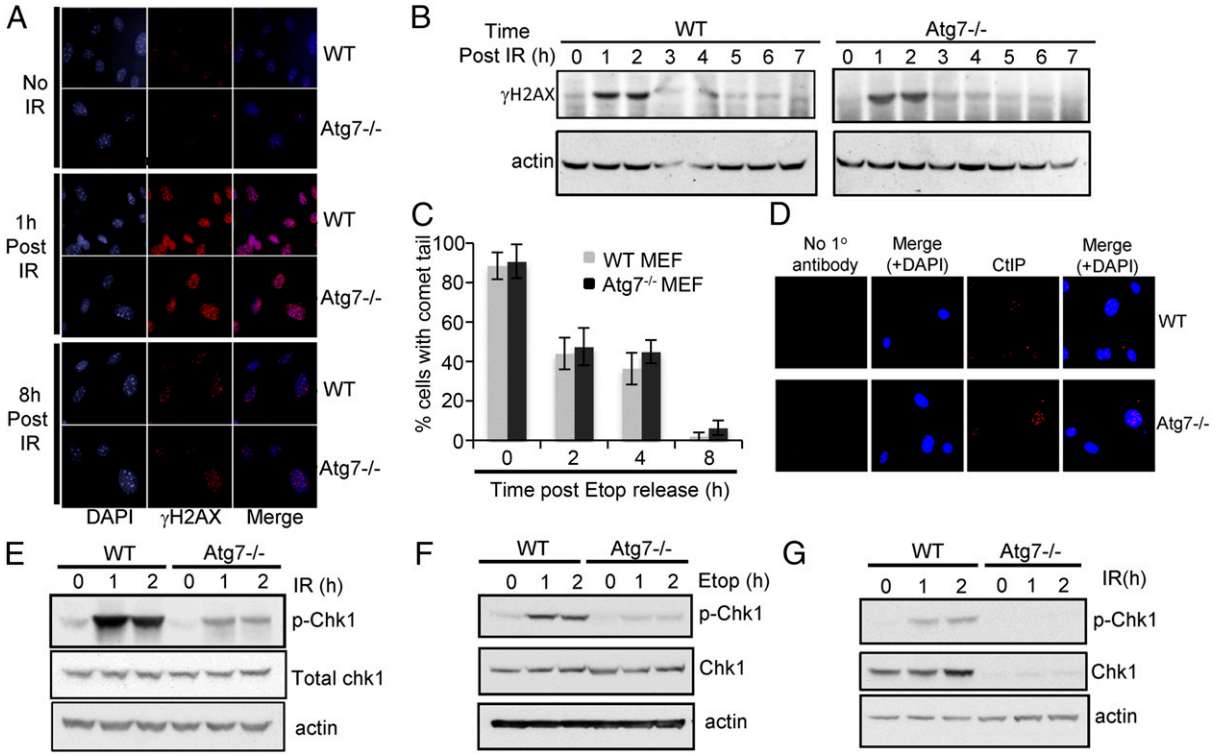

Fig. 1. Autophagy-deficient cells repair DNA double-strand breaks, but have a deficiency in Chk1. (*A* and *B*) Cell populations were irradiated (10 Gy) and assessed for accumulation of γ-H2AX by immunofluorescent detection of foci formation before, 1 h and 8 h after ionizing radiation (IR, 10 Gy) (*A*), and by Western blotting prior and at the indicated times following ionizing radiation (IR, 10,Gy) (*B*). (*C*) WT and *Atg7*$^{-/-}$ cells were treated with etoposide (Etop) for 12 h. Etop was then removed and samples were collected for comet assay at 2, 4, and 8 h after Etop release. (*D*) The subcellular localization of CtIP was assessed by immunofluorescence 1 h after irradiation (IR, 10 Gy) in wild-type and *Atg7*$^{-/-}$ cells. (*E* and *F*) Phosphorylation of Chk1 at S345 was measured by Western blotting in wild-type and *Atg7*$^{-/-}$ cells at the indicated times following exposure to 10 Gy IR or 25 μM etoposide (*F*). (*G*) Levels of phoshorylated Chk1 and total Chk1 were assessed by Western blotting following 10 Gy of ionizing irradiation in *Atg7*$^{flox/flox}$ and *Atg7*$^{-/-}$ cells that had undergone Cre-mediated recombination 2 wk previously.

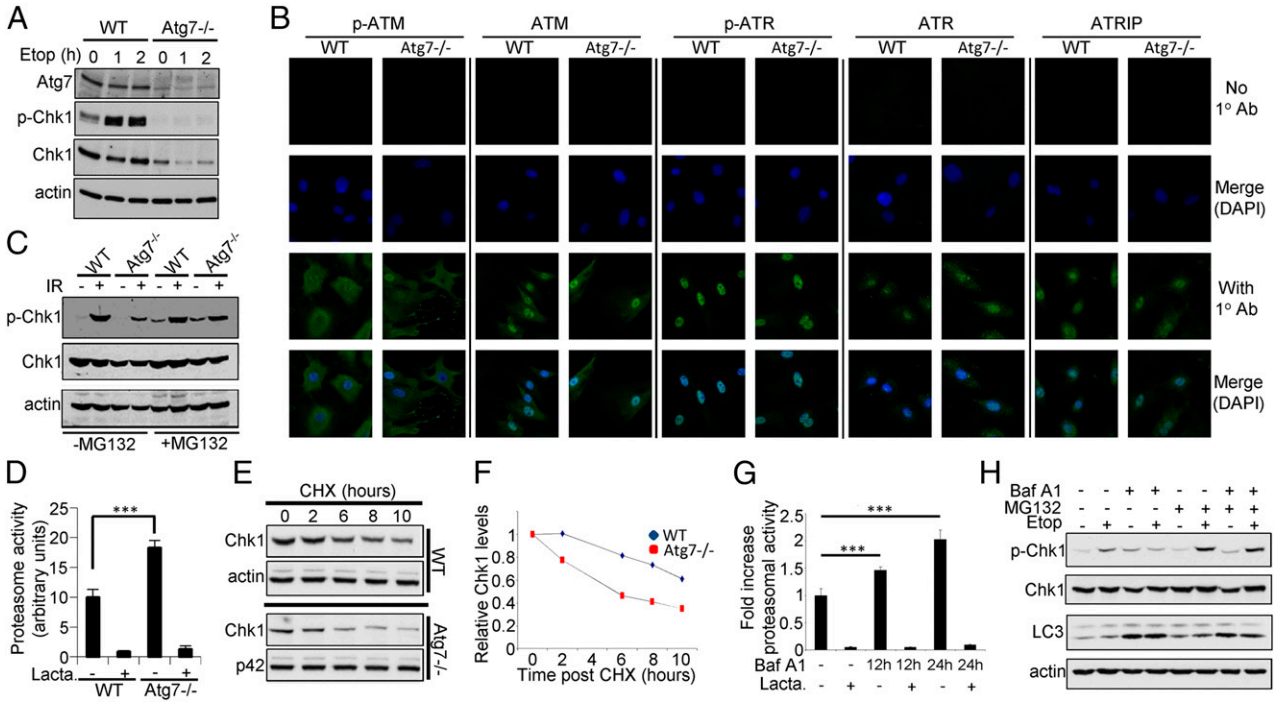

Fig. 2. The proteasomal inhibitor MG132 partially rescues phosphorylation of Chk1 at S345 in *Atg7*$^{-/-}$ cells. (*A* and *B*) Within one complete experiment, the levels of Atg7, Chk1, and p-Chk1 were measured by Western blotting in wild-type and *Atg7*$^{-/-}$ cells following treatment with 25 μM etoposide (*A*). At the same time, p-ATM, ATM, p-ATR, ATR, and ATRIP nuclear foci were assessed by immunofluorescence (*B*). For each factor, a secondary antibody-only stain was also performed (No 1° Ab) to exclude the possibility that the staining we observed was a nonspecific stain from the secondary antibody. (*C*) Chk1 activation in wild-type and *Atg7*$^{-/-}$ cells was examined 1 h post 10 Gy IR in either the absence or presence of 10 μM MG132 for 6 h. (*D*) Proteasomal activity was determined in wild-type and *Atg7*$^{-/-}$ cells using a luciferase-based assay kit. Where indicated, lactacyctin (Lacta, 10 μM) was added to the cells 3 h before harvest. Error bars indicate SD. (*E*) Endogenous Chk1 levels were determined by Western blotting in *Atg7*$^{flox/flox}$ and *Atg7*$^{-/-}$ cells, after treatment with cycloheximide (CHX, 10 μg) for various lengths of time as indicated. (*F*) Chk1 levels as shown in *E* were quantified against loading controls using ImageJ software. (*G*) Proteasomal activity was determined in cells in the presence or absence of Bafilomycin A1 (100 nM) for indicated times using a luciferase-based assay kit. Where indicated, lactacystin (10 μM) was added to the cells 3 h before harvest. Error bars represent SD. (*H*) Levels of p-Chk1 (S345) were examined by Western blotting in either the absence or presence of Bafilomycin A1 (100 nM) for 8 h and/or 10 μM MG132 for 4 h and/or etoposide (25 μM) for 4 h where indicated.

effects were not observed when wild-type MEFs were infected with Cre-recombinase (Fig. S1*E*).

We were keen to understand the mechanism responsible for the decreased levels of phospho-Chk1 in autophagy-deficient cells. We therefore measured the levels and localization of several factors involved in HR—ataxia telangiectasia mutated (ATM), p-ATM, ataxia telangiectasia and Rad3-related (ATR), p-ATR and ATR interacting protein (ATRIP)—in both wild-type cells and autophagy-deficient cells, which exhibited loss of p-Chk1 and partial loss of total Chk1 (Fig. 2*A*). There were, however, no obvious differences in the these factors between wild-type and *Atg7*$^{-/-}$ cells (Fig. 2*B*).

Because Chk1 activation is cell-cycle regulated, we also checked if there was any difference in cell-cycle distribution and S-phase entry between wild-type and Atg7-null cells. This revealed, however, that loss of autophagy had no impact on the percentage of cells at different stages of the cell cycle (Fig. S2*A*). In addition and more importantly, we also directly measured S-phase entry over time by analyzing the rate of BrdU incorporation at four time points after *Atg7* recombination. No differences were found between wild-type and autophagy-deficient cells (Fig. S2*B*).

Two factors that regulate phosphorylation and activation of Chk1 are claspin and protein phosphatase, Mg^{2+}/Mn^{2+} dependent, 1D (PPM1D/WIP1). Claspin is an adapter protein that facilitates the phosphorylation of Chk1 by ATR, and because claspin levels are known to be modulated (16), we next considered that claspin may be lower in autophagy-deficient cells. However, identical levels of claspin were observed in *Atg7*$^{-/-}$ cells and wild-type controls (Fig. S2*C*). One other possibility is that autophagy-deficient cells contain increased levels of the WIP1/PPM1D phosphatase that dephosphorylates Chk1 at S345 (17), such that even in the presence of normal phosphorylation of Chk1 by ATR, decreased total levels of p-Chk1 would be observed. However, similar to claspin, no differences in WIP1 levels were observed in autophagy-deficient cells compared with controls (Fig. S2*D*).

Previous studies have shown that Chk1 is degraded by the ubiquitin–proteasome system and that this can be stimulated by phosphorylation of the protein at S345 (18–22). Because we had observed a decrease in phospho-Chk1 at earlier time points after *Atg7* recombination, we reasoned this may be due to enhanced degradation of the protein, which over time would then have an impact on the total pool of Chk1 under conditions where DNA-damage signaling would be enhanced after a prolonged loss of autophagy. To test this hypothesis, we treated cells with the proteasome inhibitor MG132, which caused a marked increase in the levels of phospho-Chk1 that could be detected in Atg7-null cells following exposure to IR (Fig. 2*C*). In line with this effect, we also observed that autophagy-deficient cells have enhanced proteasomal activity (Fig. 2*D*), such that the half-life of phospho-Chk1 in cells lacking Atg7 is much shorter than that in wild-type cells (Fig. 2 *E* and *F*).

We were also interested to know whether loss of Chk1 through increased proteasome activity would also occur following short-term, acute autophagy inhibition, as would be the case in a therapeutic setting. To test this idea, we incubated cells with the autophagy inhibitor, bafilomycin A1, which inhibits the vacuolar ATPase at the lysosome. This revealed that treatment with bafilomycin A1 causes a progressive increase in proteasomal activity (Fig. 2*G*) and leads to a reduction in both

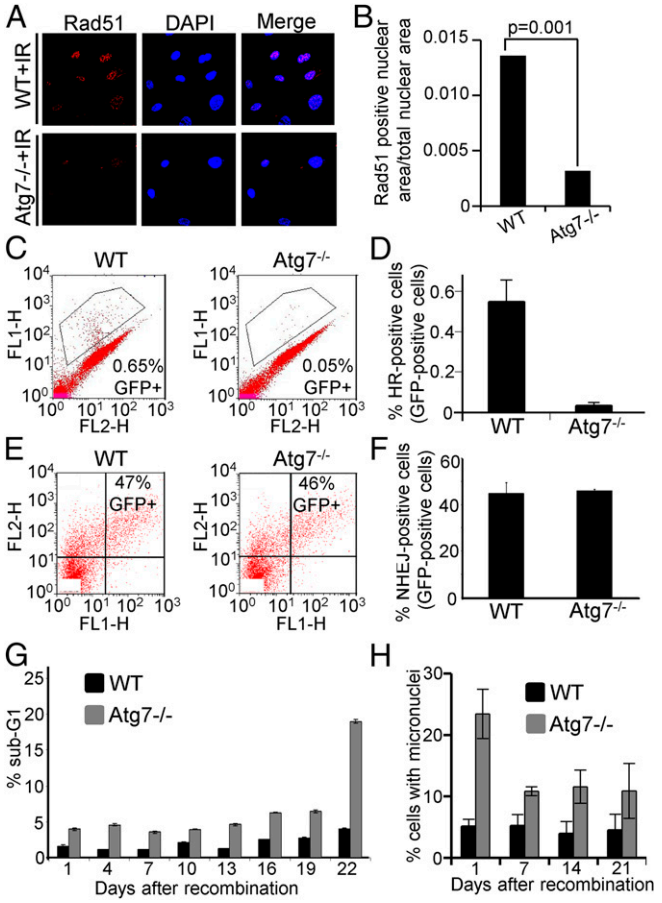

Fig. 3. Homologous recombination is impaired in autophagy-deficient cells and leads to increased cell death and mitotic aberrations. (*A* and *B*) Rad51 foci formation in the nucleus 1 h after DNA damage was assessed by immunofluorescence microscopy, in *Atg7*$^{flox/flox}$ and *Atg7*$^{-/-}$ cells (*A*). (*B*) The graph represents Rad51 positive nuclear area (foci) normalized against total nuclear area in wild-type and *Atg7*$^{-/-}$ cells. (*C*–*F*) Plasmid-based assays were used to measure HR (*C*) and NHEJ (*E*) activity in wild-type and Atg7-null cells. The profiles shown are representative of what was seen in three independent cell clones (HR assay) and in at least three independent transfections (NHEJ assay). The results of repeated experiments were quantified HR (*D*) and NHEJ (*F*). (*G*) Sub-G1 DNA content (a reliable measure of apoptotic death) was measured by flow cytometry in wild-type and *Atg7*$^{-/-}$ cells at the indicated time points after *Atg7* recombination. (*H*) Occurrence of micronuclei was examined and quantified in wild-type and *Atg7*$^{-/-}$ cells at the indicated time points after *Atg7* recombination. Error bars indicate SD, except in *G* where they represent SEM.

phospho-Chk1 and total Chk1 over time (Fig. 2*H* and Fig. S2*E*). In line with these two effects being causally related, inhibition of the proteasome with MG132 completely restored phospo- and total Chk1 levels in cells that had been treated with bafilomycin A1 (Fig. 2*H* and Fig. S2*E*).

Loss of Autophagy Impairs DNA Repair by Homologous Recombination. Although previous reports indicate that reduced Chk1 activity would theoretically lead to a deficiency in HR (13, 23), this parameter is not definitive proof that the process is impaired. We therefore tested if the diminished levels of Chk1 had functional consequence. Firstly, we tested whether Atg7-null cells were impaired in their ability to form Rad51 foci—a direct downstream readout of Chk1 activity (10, 23). This indeed revealed that autophagy-deficient cells are significantly impaired in their ability to form these foci upon DNA damage (Fig. 3 *A* and *B*). Next we directly measured HR proficiency in the absence of autophagy using previously described plasmid-based assays, which act as direct readouts of the process (24). This clearly showed that loss of autophagy has a profound effect of the ability of cells to undergo HR (Fig. 3 *C* and *D* and Fig. S3 *A* and *B*). By contrast, using plasmid assays to directly measure NHEJ (25), it was clear that autophagy-deficient cells had equivalent NHEJ activity to wild-type cells and had nuclei positive for Ku—a marker of NHEJ (Fig. 3 *E* and *F* and Fig. S4 *A* and *B*).

We also observed that autophagy-deficient cells had a decreased growth rate compared with wild-type cells (Fig. S4*C*), but this was not attributable to cell cycle arrest or decreased S-phase entry (Fig. S2 *A* and *B*). Instead, autophagy-deficient cells had higher levels of sub-G1 DNA, an indication of decreased genomic integrity, which peaked 3–4 wk after recombination of *Atg7* when the cells entered crisis (Fig. 3*G*). Furthermore, and again in line with a deficiency in HR, loss of autophagy also caused increased accumulation of micronuclei compared with wild-type controls (Fig. 3*H*).

Impaired HR in the Absence of Autophagy Reveals a Synthetic Lethal Strategy to Kill Autophagy-Deficient Cells. As outlined previously, mammalian cells have two principal mechanisms to repair DNA double-strand breaks, HR and NHEJ (10). Because autophagy-deficient cells are impaired in their ability to use HR, these cells should be hyperdependent on NHEJ. In agreement with this prediction, inhibition of DNA-PKcs (a critical component of NHEJ) following exposure to IR, resulted in impaired repair kinetics as measured by comet assay and persistence of DNA double-strand breaks as marked by γ-H2AX in autophagy-deficient cells (Fig. 4 *A* and *B* and Fig. S4 *D* and *E*). In wild-type cells, γ-H2AX foci were largely removed, presumably due to the ability of these cells to still use HR for repair under conditions of NHEJ inhibition (Fig. 4*B*).

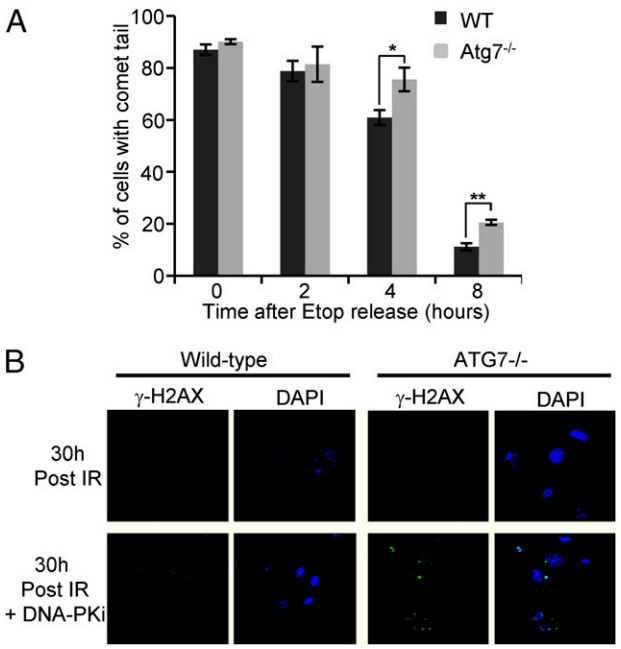

Fig. 4. Loss of autophagy impairs DNA repair kinetics upon inhibition of nonhomologous end joining (NHEJ). (*A*) WT and *Atg7*$^{-/-}$ cells were pretreated with DNA-PK inhibitor and etoposide for 12 h. Etoposide was then removed and cells were assayed for comet tail length at the indicated times. $*P < 0.05$, $**P < 0.01$. (*B*) Immunofluorescent analysis for the persistence of γ-H2AX foci 30 h after 10 Gy irradiation (IR) in control and *Atg7*$^{-/-}$ cells was assessed either in the absence or presence of 10 μM DNA-PKcs inhibitor (DNA-PKi). DAPI was used to stain DNA.

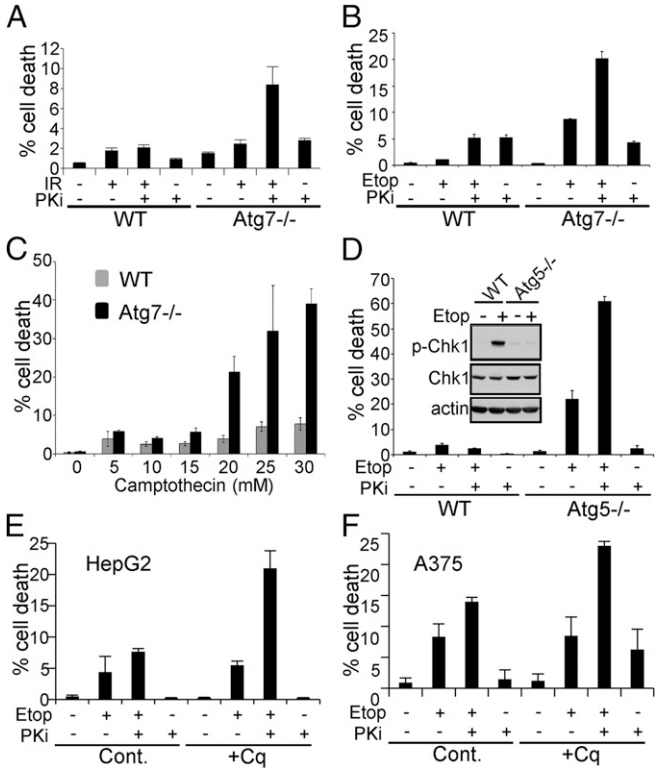

Fig. 5. Autophagy-deficient cells are hyperdependent on nonhomologous end joining (NHEJ) for cell survival. (*A* and *B*) *Atg7*$^{-/-}$ cells are hypersensitive to DNA-PKi (PKi, 10 μM) upon DNA damage induced by irradiation (10 Gy) (*A*) or treatment with etoposide (25 μM) (*B*). Cell death was assessed 24 h after irradiation and 48 h after treatment with etoposide. Total cell populations were collected and assessed for sub-G_1 DNA content by flow cytometry. (*C*) Wild-type and *Atg7*$^{-/-}$ cells were treated with indicated concentrations of camptothecin for 16 h and cell death was accessed by flow cytometry analysis of sub-G1 DNA content. (*D*) *Atg5*$^{flox/flox}$ MEFs were infected with Cre-recombinase or empty retroviral vector as contol. Following selection, cells were, where indicated, exposed to etoposide and/or DNA-PKi for 48 h. Total cell populations were collected and assessed for sub-G_1 DNA content by flow cytometry. At 1 h after treatment with etoposide, cell lysates were also analyzed for Chk1 phosphorylation at S345 by Western blotting (*D*, *Inset*). (*E* and *F*) The autophagy inhibitor chloroquine sensitizes HepG2 and A375 cells to cell death upon treatment with DNA-PKi (PKi, 2 μM) and etoposide (25 μM). At 48 h after treatment with etoposide, total cell populations were collected and assessed for sub-G_1 DNA content by flow cytometry. Error bars indicate SD.

We hypothesized that the persistence of DNA damage in autophagy-deficient cells may result in programmed cell death, such that induction of DNA double-strand breaks in combination with DNA-PKcs inhibition, may represent a selective synthetic lethal situation for the killing of autophagy-deficient cells. Indeed when cells were treated with a DNA-PKcs inhibitor (DNA-PKi) before 10 Gy IR, a marked synergistic killing was observed in autophagy-deficient cells (Fig. 5*A*), whereas no synergy was observed in wild-type cells (Fig. 5*A*). Although no difference in radiosensitivity was observed with 10 Gy in the absence of DNA-PKi, Atg7-null cells were, as would be expected, inherently more sensitive to higher doses of IR (25 Gy) (Fig. S5*A*).

Decreased levels of activated phospho-Chk1 were also observed in autophagy-deficient cells treated with etoposide—a therapeutic agent that inhibits topoisomerase and causes DNA double-strand breaks (Fig. 1*F*). Autophagy-deficient cells were already more sensitive to etoposide than wild-type controls and the combination of etoposide with DNA-PKi, similar to what was observed following exposure to IR, resulted in selective synergistic killing of *Atg7*$^{-/-}$ cells (Fig. 5*B*).

To confirm these results and to test if this synthetic lethal situation exists in a different cell system, we examined MEFs from SCID mice, which have an inactivating mutation in *DNA-PKcs* (26). This revealed in line with our previous observations that synergistic killing can be achieved in these cells by treatment with etoposide and an inhibitor of autophagy (Fig. S5*B*). Moreover, intrinsic cell death sensitivity was also observed when Atg7-null MEFs were treated with the chemotherapeutic drug camptothecin, which induces genetic lesions that can only be repaired by HR (27), underscoring again that this process of DNA repair is impaired in the absence of autophagy (Fig. 5*C*).

We were also keen to ascertain whether the effects we observed were related to autophagy or more specifically just to Atg7. MEFs were therefore isolated from mice containing a floxed allele for *Atg5* (another essential autophagy gene) and were infected with Cre or control virus as before (Figs. S1*A* and S5*C*). This revealed, similar to what was observed with Atg7, that loss of Atg5 also resulted in diminished levels of phospho-Chk1 (Fig. 5*D*, *Inset*). In addition, these cells were also intrinsically sensitive to etoposide and when inhibition of DNA-PKcs was combined with etoposide treatment, a significant synergy in cell death induction was clearly evident in *Atg5*$^{-/-}$ cells, whereas no synergy was again seen in wild-type cells (Fig. 5*D*).

Lastly, from a potentially clinical perspective, we sought to determine if chemical inhibition of autophagy could sensitize tumor cells to etoposide when cultured in the presence of DNA-PKi. To test this hypothesis, we treated cells with the lysosomotropic agent chloroquine which inhibits the turnover stage of autophagy. In line with our MEF data, this revealed that choroquine enhances etoposide-induced cell death in some cells (HepG2 and A375) when DNA-PK is inhibited, but no impact on the viability of these cells was observed when treated with etoposide in the absence of DNA-PKi (Fig. 5 *E* and *F*). We found, however, that this was not a general phenomenon because chloroquine had no effect on cell death in other cells (Fig. S5*D*).

Discussion

When taken together, the findings we present in this study mechanistically connect two important areas of biology—autophagy and DNA repair. We show that loss of autophagy results in decreased levels of phospho-Chk1, which at later time points after recombination of essential autophagy genes, also affects total Chk1 levels. We propose that the decreased levels of Chk1 in the absence of autophagy are due to increased proteasomal activity, which leads to a decrease in the half-life of Chk1 when its degradation is signaled through phosphorylation at serine 345. In line with this conclusion, we show that the levels of Chk1 can be restored by treatment with the proteasomal inhibitor MG132. Although our data are consistent with this mechanism, it must be considered that due to the far-reaching effects of autophagy, there may potentially be other perturbations in autophagy-deficient cells that also affect Chk1 levels or indeed, HR in a Chk1-independent manner. In this regard, while we did not detect any differences in the upstream signaling pathways that lead to Chk1 activation, because Chk1 phosphorylation is mechanistically connected to Chk1 degradation, it remains possible that these pathways are in some way altered in autophagy-deficient cells and that at some level, when combined with enhanced proteasomal activity, this contributes to Chk1 loss.

Stimulated by our data with Chk1, we categorically show that autophagy-deficient cells are impaired in DNA repair by the error-free process, homologous recombination. As a result, the greater dependency of autophagy-deficient cells on the error-prone repair process of NHEJ, could at least in part explain the previously described accumulation of DNA damage in autophagy-deficient cells (5, 28), because sustained reliance on NHEJ

will result in loss of nucleotides and chromosome translocations. These findings therefore highlight yet another mechanism by which the loss of autophagy can compromise cellular integrity and viability, and we consider that this may be particularly relevant when we consider that autophagy inhibitors are being developed for clinical use. In this regard, it is particularly noteworthy that we could reduce the levels of activated Chk1 with only short-term treatment with an autophagy inhibitor (Fig. 2*H*) and that this may theoretically result in genomic damage if used over a protracted period.

In terms of therapy, we also show that genetic loss or chemical inhibition of autophagy creates a synthetic lethal situation in some cells when inhibition of NHEJ is combined with induction of DNA double-strand breaks. This is, to the best of our knowledge, the first theoretical strategy for the selective killing of autophagy-deficient cells. Therefore, the findings we present in this report not only provide important insights into the consequence of autophagy inhibition on DNA repair, but they may also aid in the development of new therapeutic strategies that exploit the fact that autophagy-deficient cells have impaired HR and a resultant hyperdependency on NHEJ.

Materials and Methods

Cell Culture. *Atg7*$^{flox/flox}$ mice were kindly provided by Masaaki Komatsu, Niigata University, Niigata, Japan, and have been previously described (29). *Atg5*$^{flox/flox}$ mice were from RIKEN and have also been previously described (30). Primary MEFs were isolated from embryonic day (E)13.5–E14.5 mouse embryos. All cells were grown in DMEM (Invitrogen) supplemented with 10% (vol/vol) FBS and were maintained at 37 °C in an atmosphere of 5% (vol/vol) CO_2 in air.

Retroviral Infections. pBabe-Puro-Cre was generated by PCR amplification and was cloned into the EcoRI and SalI sites of pBabe-puro. Primary MEFs were infected with pBabe-puro-Cre or pBabe-puro as control as previously described (31). Cells were then selected in 2.5 μg/mL puromycin for 3 d.

Western Blotting. Cells were lysed in radioimmunoprecipitation assay (RIPA) buffer and transferred to nitrocellulose or immobulin-P membranes as previously described (32). Membranes were probed using standard immunoblotting techniques with antibodies that recognize S345 p-Chk1 (Cell Signaling, 2348), total Chk1 (Santa Cruz, sc8404), Claspin (H300; Santa Cruz, sc48771), LC3B (Cell Signaling, NB100-2331H), ERK p42 (Santa Cruz, sc154), Wip1 (Santa Cruz, sc20712), γ-H2AX (Millipore, 05636), HA (Cell Signaling, 2367), and actin (clone 1A4; Sigma, ab8227). All Western blots shown are representative of what was observed in at least three independent experiments.

Immunofluorescence. Immunofluorescence was undertaken as described in *SI Materials and Methods*. Primary antibodies used were γ-H2AX (1:250; Millipore, 05636), Rad51 (1:1,000; Calbiochem, PC130), CtIP (1:100; Cell Signaling, 9201), S1981 p-ATM (Rockland Immunochemicals, 200301500), total ATM (Oncogene Research, PC116), KU-70 (Santa Cruz, sc1487), ATR (1:100; Santa Cruz, sc1887), p-ATR (1:100; Santa Cruz, sc109912), ATRIP (1:100; Bethyl Laboratory, A300-095A), and HA (1:100; Cell Signaling, 2367). Secondary antibodies used were Alexa Fluor 488 or Texas Red conjugates (Invitrogen). Images were captured using a confocal microscope (A1R Nikon or FV1000 Olympus) using either a Plan-Apochromat VC60× N.A. 1.40 oil or UPLSAPO 60× N.A. 1.35 oil objective together with NIS-Elements AR Nikon or Fluoview version 1.7c Olympus software, respectively.

qRT-PCR. RT-qPCR analysis was undertaken using the DyNAmo SYBR Green 2-step qRT-PCR kit (Finnzymes). Data collection was carried out using a Chromo4 real-time PCR detector and analyzed with Opticon Monitor 3. Primers for qPCR reactions were as follows: Atg7: 5′-ATGCCAGGACACCCTGTGAACTTC-3′ and 5′-ACATCATTGCAGAAGTAGCAGCCA-3′; Atg5: 5′-AAGTCTGTCCTTCCGCAG-3′ and 3′-TGAAGAAAGTTATCTGGGTAG-5′. Mouse 18S primers were from Qiagen (QT01036875).

Cycling parameters were 95 °C 15 min, (94 °C 10 s, 55 °C 30 s, 72 °C 30 s) 40 cycles, 72 °C 10 min. Expression levels of genes analyzed by qPCR were normalized relative to levels of 18S rRNA.

Analysis of Proteasome Activity. The proteasome assays were performed after treatment of wild-type MEFs with 100 nM Bafilomycin A1 for 16 h, and/or with Lactacystin (10 μM) for 2 h where indicated. The assays were performed using Proteasome-Glo Cell-Based Reagents (Promega Bioscience) according to the manufacturer's instructions.

ACKNOWLEDGMENTS. We thank Masaaki Komatsu and Noboru Mizushima (RIKEN) for mice used to generate *Atg7*$^{fl/fl}$ MEFs and *Atg5*$^{fl/fl}$ MEFs, respectively, Vera Gorbunova and Kevin Hiom for DNA repair reagents, and Tony McBryan for help with statistics. This work was supported by Cancer Research UK and the Association for International Cancer Research.

1. Xie Z, Klionsky DJ (2007) Autophagosome formation: Core machinery and adaptations. *Nat Cell Biol* 9(10):1102–1109.
2. Cadwell K, Stappenbeck TS, Virgin HW (2009) Role of autophagy and autophagy genes in inflammatory bowel disease. *Curr Top Microbiol Immunol* 335:141–167.
3. Rosenfeldt MT, Ryan KM (2009) The role of autophagy in tumour development and cancer therapy. *Expert Rev Mol Med* 11:e36.
4. Wong E, Cuervo AM (2010) Autophagy gone awry in neurodegenerative diseases. *Nat Neurosci* 13(7):805–811.
5. Karantza-Wadsworth V, et al. (2007) Autophagy mitigates metabolic stress and genome damage in mammary tumorigenesis. *Genes Dev* 21(13):1621–1635.
6. Kroemer G, White E (2010) Autophagy for the avoidance of degenerative, inflammatory, infectious, and neoplastic disease. *Curr Opin Cell Biol* 22(2):121–123.
7. Hoeijmakers JH (2009) DNA damage, aging, and cancer. *N Engl J Med* 361(15): 1475–1485.
8. Jackson SP, Bartek J (2009) The DNA-damage response in human biology and disease. *Nature* 461(7267):1071–1078.
9. Olive PL, Banáth JP (2006) The comet assay: A method to measure DNA damage in individual cells. *Nat Protoc* 1(1):23–29.
10. Sancar A, Lindsey-Boltz LA, Unsal-Kaçmaz K, Linn S (2004) Molecular mechanisms of mammalian DNA repair and the DNA damage checkpoints. *Annu Rev Biochem* 73: 39–85.
11. Mimitou EP, Symington LS (2009) DNA end resection: Many nucleases make light work. *DNA Repair (Amst)* 8(9):983–995.
12. You Z, Bailis JM (2010) DNA damage and decisions: CtIP coordinates DNA repair and cell cycle checkpoints. *Trends Cell Biol* 20(7):402–409.
13. Sørensen CS, et al. (2005) The cell-cycle checkpoint kinase Chk1 is required for mammalian homologous recombination repair. *Nat Cell Biol* 7(2):195–201.
14. Smith J, Tho LM, Xu N, Gillespie DA (2010) The ATM-Chk2 and ATR-Chk1 pathways in DNA damage signaling and cancer. *Adv Cancer Res* 108:73–112.
15. Baldwin EL, Osheroff N (2005) Etoposide, topoisomerase II and cancer. *Curr Med Chem Anticancer Agents* 5(4):363–372.
16. Peschiaroli A, et al. (2006) SCFbetaTrCP-mediated degradation of Claspin regulates recovery from the DNA replication checkpoint response. *Mol Cell* 23(3):319–329.
17. Lu X, Nannenga B, Donehower LA (2005) PPM1D dephosphorylates Chk1 and p53 and abrogates cell cycle checkpoints. *Genes Dev* 19(10):1162–1174.
18. Zhang YW, et al. (2005) Genotoxic stress targets human Chk1 for degradation by the ubiquitin-proteasome pathway. *Mol Cell* 19(5):607–618.
19. Collis SJ, et al. (2007) HCLK2 is essential for the mammalian S-phase checkpoint and impacts on Chk1 stability. *Nat Cell Biol* 9(4):391–401.
20. Feng JM, Zhu H, Zhang XW, Ding J, Miao ZH (2008) Proteasome-dependent degradation of Chk1 kinase induced by the topoisomerase II inhibitor R16 contributes to its anticancer activity. *Cancer Biol Ther* 7(11):1726–1731.
21. Leung-Pineda V, Huh J, Piwnica-Worms H (2009) DDB1 targets Chk1 to the Cul4 E3 ligase complex in normal cycling cells and in cells experiencing replication stress. *Cancer Res* 69(6):2630–2637.
22. Zhang YW, et al. (2009) The F box protein Fbx6 regulates Chk1 stability and cellular sensitivity to replication stress. *Mol Cell* 35(4):442–453.
23. Suwaki N, Klare K, Tarsounas M (2011) RAD51 paralogs: Roles in DNA damage signalling, recombinational repair and tumorigenesis. *Semin Cell Dev Biol* 22(8):898–905.
24. Pierce AJ, Johnson RD, Thompson LH, Jasin M (1999) XRCC3 promotes homology-directed repair of DNA damage in mammalian cells. *Genes Dev* 13(20):2633–2638.
25. Seluanov A, Mittelman D, Pereira-Smith OM, Wilson JH, Gorbunova V (2004) DNA end joining becomes less efficient and more error-prone during cellular senescence. *Proc Natl Acad Sci USA* 101(20):7624–7629.
26. Blunt T, et al. (1996) Identification of a nonsense mutation in the carboxyl-terminal region of DNA-dependent protein kinase catalytic subunit in the scid mouse. *Proc Natl Acad Sci USA* 93(19):10285–10290.
27. Arnaudeau C, Lundin C, Helleday T (2001) DNA double-strand breaks associated with replication forks are predominantly repaired by homologous recombination involving an exchange mechanism in mammalian cells. *J Mol Biol* 307(5):1235–1245.
28. Mathew R, et al. (2007) Autophagy suppresses tumor progression by limiting chromosomal instability. *Genes Dev* 21(11):1367–1381.
29. Komatsu M, et al. (2005) Impairment of starvation-induced and constitutive autophagy in Atg7-deficient mice. *J Cell Biol* 169(3):425–434.
30. Hara T, et al. (2006) Suppression of basal autophagy in neural cells causes neurodegenerative disease in mice. *Nature* 441(7095):885–889.
31. Helgason GV, O'Prey J, Ryan KM (2010) Oncogene-induced sensitization to chemotherapy-induced death requires induction as well as deregulation of E2F1. *Cancer Res* 70(10):4074–4080.
32. Bell HS, et al. (2007) A p53-derived apoptotic peptide derepresses p73 to cause tumor regression in vivo. *J Clin Invest* 117(4):1008–1018.